Research Article Adv. Mater. Lett. 2015, **6**(8), 690-694 Advanced Materials *Letters*

www.amlett.com, www.vbripress.com/aml, DOI: 10.5185/amlett.2015.5822 Published online by the VBRI Press in 2015

Competition between layering & nano-clustering of indium atoms on reconstructed Si (113) 3x2 surface

Shibin T. C. Krishna[1,2], Prachi Rastogi[2], Neha Aggarwal[1,2], Amit Kumar Singh Chauhan[2], Mukesh Kumar[2], Govind Gupta[1,2]*

[1]*Academy of Scientific & Innovative Research (AcSIR), CSIR-National Physical Laboratory (CSIR-NPL) Campus, Dr. K. S. Krishnan Road, New Delhi 110012, India*
[2]*Physics of Energy Harvesting, CSIR-National Physical Laboratory (CSIR-NPL), Dr. K.S. Krishnan Road, New Delhi 110012, India*

*Corresponding author. Tel: (+91)- 11-45608403; (+91)-11-45609310, Email. govind@nplindia.org

Received: 29 January 2015, Revised: 15 March 2015 and Accepted: 20 March 2015

ABSTRACT

Scanning tunneling microscopy and X-ray photoelectron spectroscopy have been utilized to probe the growth kinetics, phenomenon of nucleation and segregation of Indium nano-islands on atomically clean stepped Si (113) 3x2 surface. Kinetically controlled growth of few monolayers (2.5 ML) of Indium (In) atoms at room temperature leads the formation of two dimensional (2D) nanoclusters on Si (113) surface. The thermal stability of these In nanoclusters was investigated by residual thermal desorption experiments where the In adsorbed system was annealed at different temperatures (100-600^{o}C). It is found that, the size and density of the In nanoclusters on Si surface were influenced by the annealing temperature. In particular, on annealing the In/Si (113) system at 300°C, 2D nanoclusters were converted into a metastable state of 3D nanoclusters. Competition between layering and nano-clustering has been observed twice during the entire thermal annealing process and discussed in detail. The size tunability of these metal nanoclusters on silicon surfaces could be utilized for the fabrication of next generation nanoscale devices.

Keywords: Indium; Si (113); STM; nanocluster.

Introduction

Metal nano-clusters (NCs) are promising material in the area of optoelectronic devices due to their superior optical & structural properties [**1, 2**]. The growth of metal NCs can be achieved by numerous techniques such as photolithography [**3**], sub-lithography [**4**], scanning probe tip [**5**], ion beam sputtering [**6**], molecular beam epitaxy etc. However, it can naturally be achieved by the phenomena of i) self-assembly, where surface reconstructions [**7**] play a significant role to create metallic nano-structures and ii) lattice mismatched strain, which can be utilized to grow epitaxial nanowires [**8**]. The success of metal NCs for futuristic device applications will strongly depend on the availability of three, two- or one-dimensionally organized materials [**9, 10**]. So the understanding of growth conditions of metal NCs and their size tunability is essential to utilize them in the fabrication of next generation nanoscale devices. Further, the size of the metal NCs not only depends on the growth techniques and conditions, but also can be altered by post growth sputtering or annealing treatments. There have been a number of reports on the formation of size dependent NCs compounds by means of sputtering and post annealing treatments [**11-13**].

The growth of metal NCs on Silicon (Si) surfaces has attracted scientific and technological attention because of their easy availability and cost effectiveness [**14**]. There are many studies of metal NCs growth on low index/planar silicon surfaces, such as Si (100) and Si (111) surfaces [**7, 8**]. However, there have been few reports of metal growth on high index/stepped silicon surface, such as Si (557) and Si (5512) surfaces [**15, 16**]. Among high-indexed surfaces, a clean Si (113) is a stepped surface, thermally more stable and good substrate for epitaxial growth [**17**].

Fig. 1 shows the cross-sectional schematic view of the bulk silicon cut perpendicular to the [$33\bar{2}$] direction along with high index orientation planes at different angle. III-group elements (like Ga, In) have become promising candidates for the surfactant mediated epitaxy [**18, 19**], therefore, the growth of these elements on silicon surfaces has attracted much interest for availing initial understanding of high quality III-V based semiconductors. There have been few reports on Ga, Al adsorption on reconstructed Si (113) 3x2 surface [**20, 21**] which lead to the formation of various superstructural phase formations on reconstructed

Si (113) surface. Conversely, the growth of In on Si (113) surface is not premeditated. Recently, the growth of In metal atoms on Si (113) surface has been studied by our group [**11**] where the formation of In induced various superstructural phases on Si (113) has been reported. In view of future nanoscale device applications, a comprehensive knowledge of self-assembly and the epitaxial process becomes mandatory for any dedicated growth of low dimensional structures.

(hkl)	θ°
001	0
113	25.2
55 12	30.5
337	31.2
553	42.43
111	54.7

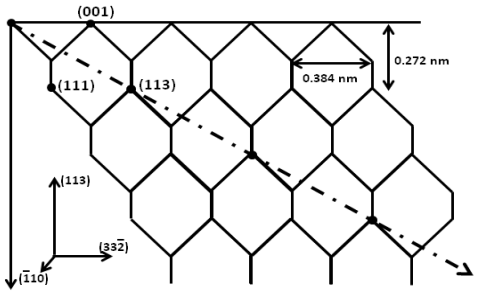

Fig. 1. Schematic diagram for various facets of Si surface with high index orientation planes at different angles.

In the present study, an intensive analysis is performed to understand the nucleation, segregation and surface morphology of In metal atoms on reconstructed Si (113) 3x2 surface via scanning tunneling microscopy. Interestingly, the size tunability of the In-metal NCs as a function of substrate temperature has been observed and discussed in detail. During the thermal desorption process, a competition between layering and clustering of In metal nanoclusters on Si (113) surface has been examined and correlated with our previous report.

Experimental

The experiments (Indium adsorption and desorption) were performed in an Omicron-Multiprobe Surface Analysis System with a base pressure of $5x10^{-11}$ Torr. Modified Shiraki process [**22**] was adopted for ex-situ cleaning of the Si (113) sample (p-type, B-doped, resistivity 0.5 Ω/cm, size ~20x8x0.35 mm^3, Vin karola, USA) before inserting it into the Ultra High Vacuum (UHV) system. The sample is mounted on a high precision four axis manipulator that enables its positioning for growth and analysis. Sample heating (direct and resistive mode), from 30°C to 1100°C, was monitored by a W–Re 5%–25% thermocouple calibrated with an optical pyrometer. Si (113) sample was annealed at 500°C for four hours, followed by flashing at 1100°C (5 Sec) and slowly cooled down to room temperature resulting in an atomically clean surface Si (113) with impurity levels below the detection limit. Indium metal (99.999%, from CERAC, USA) was evaporated from a homemade Tantalum Knudsen cell at a desired flux rate by circulating the current. The adsorption and desorption process was monitored by X-ray Photoelectron Spectroscopy (XPS, OMICRON, France) with a hemispherical electron energy analyzer and Mg K_α (1253.6 eV) source. Omicron UHV-Scanning Tunneling Microscope (STM) was used to probe the surface morphology of In/Si (113) system. The residual thermal desorption (RTD) experiments have been carried out by keeping the sample at a particular temperature for 1 min followed by XPS and STM measurement. All STM images were taken at RT. As for the way STM images were taken, they were not taken consecutively. Therefore, the same area was not observed in a series of STM images.

Results and discussion

The chemical composition of the clean Si (113) 3x2 reconstructed surface is determined by XPS analysis. **Fig. 2(a)** shows the XPS-survey scan of atomically clean Si (113) surface which exhibit peaks at binding energies 99.8 eV and 150.0 eV corresponding to Si (2p) and Si (2s) peaks respectively along with a very tiny peak at 284.6 eV associated to Carbon (1s) spectra. No peak corresponding to oxygen was observed in the XPS spectra which elucidate the cleanliness of the Si surface. In F**ig. 2(b)**, the surface morphology of atomically clean Si (113) surface is displayed where the large area STM image reveals that the surface is uniformly steeped with large terraces having an average terrace width of about 40 nm. For better understanding of terrace orientation and step height, corresponding 3D image is shown in **Fig. 2(c)**. The measured step height of the terraces was ~ 0.8 nm while the angle between every adjacent terrace was found to be 56°. These obtained values (terrace width: 40 nm, step height: 0.8 nm) are found to be in good agreement with the values of terrace width and step height reported by Dijken *et.al.* [**23**]. Inset of F**ig. 2(b)** displays row like atomic arrangement of 3x2 reconstructed Si (113) surface which shows some missing protrusion, leaving vacancies in the atomic arrangement due to the moved adatoms from Si (113) surface. The unit cell of Si (113) 3x2 reconstruction is shown in a frame in the inset of **Fig 2(b)**.

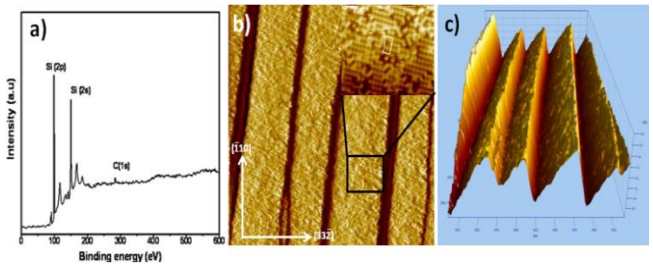

Fig. 2. (a) XPS survey scan of the clean Silicon (113) 3x2 reconstructed surface, (b) STM image of Si (113) 3x2 reconstructed surface at 200x200nm^2 scan area, Inset show 20x20nm^2 scan (I=600 pA, V_t=0.7V) and (c) corresponding 200x200nm^2 scan area 3D image (I=700 pA, Tip voltage (V_t)=0.9V).

There have been several reports on the reconstruction of Si (113) surface [**24-28**] where the phase transition from 1x1 to stable 3x2 reconstructions has been explained. Schreiner *et al.* [**29**] observed 3x1 and 3x2 surface reconstructions after annealing the Si (113) surface in the temperature range 200°C-700°C. Sequential observation of 3x1 and 3x2 phases with increasing annealing temperature indicates that the 3x1 phase is a metastable state and 3x2 phase is the most stable reconstructed phase observed at room temperature (RT). Siebert *et al.* [**30**] have also shown that 3×2 reconstructed surface is more stable than other reconstructions due to the lower average energy per atom (−4.775 eV). Here, the atomically clean reconstructed Si (113) 3x2 surface (**Fig. 2b**) has been utilized for the

kinetically controlled growth of In metal atoms at room temperature with a very low flux rate of 0.08 ML/min, which follows layer-by-layer growth mode (Frank-van der Merve). The detail of complete growth kinetics is given elsewhere **[11].**

Fig. 3(a) represents the XPS survey scan of clean Si (113) surface covered with 2.5ML of In metal atoms grown at RT where two additional peaks at binding energies 444.0 eV and 451.4 eV were observed, which corresponds to In ($3d_{5/2}$) and In ($3d_{3/2}$) peaks along with Si (2s) and Si (2p) peaks at 99.8 eV and 150.0 eV respectively. The XPS core level spectra of In ($3d_{5/2}$) of In/Si (113) structure is shown in inset the of **Fig. 3(a)**. In ($3d_{5/2}$) spectra is deconvoluted into two components: the component at Binding Energy (BE) 443.9 eV displays the presence of In-In bond (metallic indium) and peak at 445.2eV can be attributed to inelastic losses to the conduction electrons in the charge accumulation layer [**31**]. **Fig. 3**(**b**) shows the surface morphology of 2.5 ML covered In on Si (113) surface grown at RT. The surface shows tiny two dimensional NCs on top of the 2ML covered In on Si (113) surface. The surface terraces were clearly observable in the grown surface, where there is a slight reduction in step bunching value (0.4 nm) which could be due to the occupation of In metal NCs at the edge of the steps in order to stabilize the surface free energy, leads to drop in the actual step bunching value. For exact evaluation of cluster size and the variation in the step bunch with temperature, corresponding 3D image is shown in **Fig. 3(c)**. The calculated average cluster density and size of these 2D-NCs is found to be 5 E12 cm^{-2} and 6±0.3 nm, respectively.

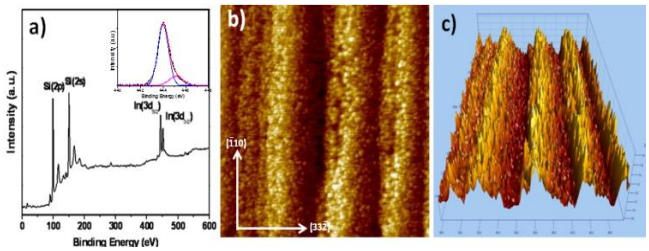

Fig. 3. (a) XPS survey scan of room temperature In adsorbed Si (113) surface. Inset shows the deconvoluted $In3d_{5/2}$ core level spectra, (b) STM image (200x200 nm^2) of In covered Si(113) 3x2 surface and (c) corresponding 3D image (I=700 pA, V_t=0.9V).

The thermal stability and morphological evolution of layer-by-layer grown In/Si (113) system has been analyzed by the residual thermal desorption method where In covered Si (113) system was subject to annealing at different temperatures (from 100 to 600° C) for a fixed time (1 min). It was observed that the size and density of the In clusters on Si surface were influenced by the annealing temperature, as shown in **Fig. 4(a-f)**. 3D images of corresponding STM image have been shown in **Fig. 4(i-vi)**. On annealing the In/Si (113) surface at 100°C, no significant change in the surface morphology was observed apart from slight temperature driven rearrangement of In atoms on the surface. A size variation in the NCs was observed as compared to the RT deposited system. The average cluster density and size of these 2D-NCs is found to be 7 E12 cm^{-2} and 4.5±0.3 nm, respectively. On increasing the substrate temperature to 200°C, density of 2D-NCs reduces significantly and a flat surface morphology was observed. This could be due to the complete desorption of loosely bound In atoms from bilayer leaving with very tiny NCs (cluster density: 1.2 E13 cm^{-2}, size: 2±0.3nm) on the surface. It can be explained as follows: initially In NCs are separated into smaller nanoislands due to temperature driven mobility (segregation) and on further increasing the annealing temperature, evaporation of these smaller nanoislands took place. A Similar trend of rearrangement of In atoms was observed by Auger Electron Spectroscopy (AES) analysis [**12**] where the In/Si AES intensity ratio decreases with increasing temperature. This illustrates the initial desorption of partial monolayer from the In/Si (113) surface.

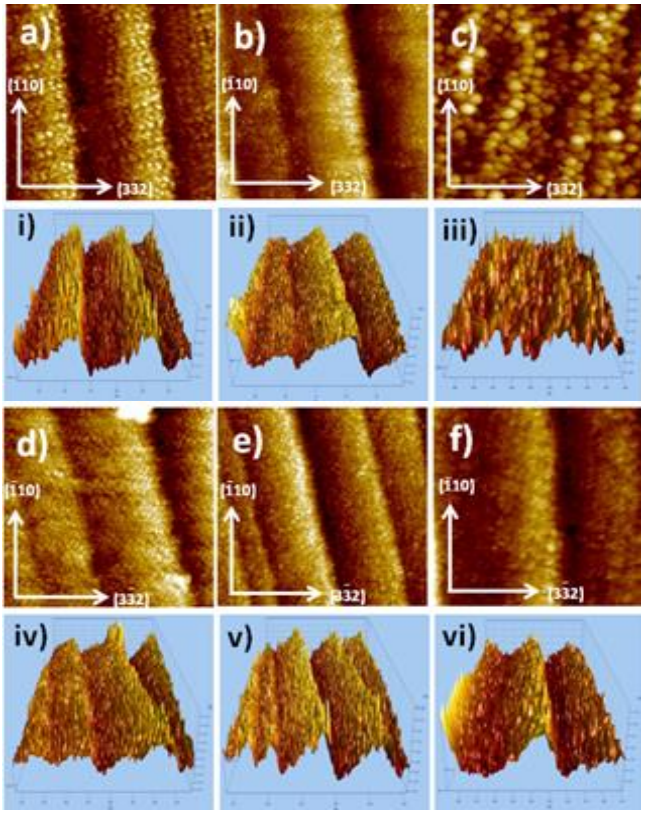

Fig. 4. STM image (100x100 nm^2) shows the morphological changes of deposited indium on Silicon (113) 3x2 reconstructed surface subjected to annealing at temperatures (a) 100 °C, (b) 200 °C, (c) 300 °C, (d) 400 °C, (e) 500 °C and (f) 600 °C, (i)-(vi) corresponding 3D images (I=700 pA, V_t=0.9V).

On annealing the In/Si(113) surface at 300° C, it was observed that the surface is fully covered with Indium 3D spherical nanoclusters (SNCs). The average size and density of these SNCs is calculated to be 10±0.3 nm and 2E12 cm^{-2} respectively. Annealing at this temperature (300° C) provides more mobility to the surface atoms to nucleate themselves and allow to form SNCs. A similar trend of temperature-induced rearrangement of In atoms was also observed in planar Si (111) 7x7 **[32]** and trenched Si (5512) 2x1 **[14]** surfaces where the conversion of 2D layer into 3D island has been observed. Goswami *et al.* **[33]** explained that under the favorable condition, atoms agglomerate in larger cluster size/preferred size by the

quantum size effects in metallic overlayer. There could be a possibility of Si atoms residing at the interstitial site migrate to the surface and cause the formation of indium–silicon bonds. However, the deconvoluted In ($3d_{5/2}$) core level spectra (not shown here) decline the possibility of In-Si bond formation. On annealing In/Si (113) system at 400^o C, the STM image show tiny 2D-NCs (**Fig. 4(d)**) on Si (113) surface having an average size of 2.5±0.3 nm and cluster density of 1.1 E13 cm^{-2}. Here, we observed the conversion of 3D-SNCs into 2D-NCs on top of the surface. This interesting temperature induced conversion of 3D SNCs to 2D- NCs can be explained either due to desorption of atomic layer or temperature driven enhanced mobility which causes atomic rearrangements. Our previous report **[12]** confirmed that at annealing temperature above 350^{o}C signifies desorption of bilayer (In-In bond) and the formation of a stable monolayer on the Si (113) surface. In view of this, STM image at 400^o C annealing shows Si (113) surface having 1ML coverage of tiny 2D-In metallic NCs.

Table 1. Calculated average size and density of In NC subjected to annealing at different temperatures.

Annealing Temperature (^{o}C)	Average Nanocluster size (nm)	Nanocluster Density (x10^{12}cm^{-2})
RT deposited	6 ±0.3	5
100	4.5±0.3	7
200	2±0.3	12
300	10±0.3	2
400	2.5±0.3	11
500	2±0.3	9
600	4±0.3	4

On annealing the In/Si (113) at 500^o C, a flat overlayer of In on Si (113) surface was observed as shown in **Fig. 4(e)**. A similar surface morphology has also been observed at annealing temperature 200° C which shows the flat bilayer (In-In) covered Si (113) surface. In both the cases, initially 2D-NCs are segregated on the surface by the effect of temperature and finally converted into a stable and smooth In flat-layer on the Si (113) surface. Here, the transformation of surface morphology from 2D-NCs to flat overlayer of In was ensued. This unusual phenomenon occurred may be because of the gradual reduction in the strain of In/Si (113) system which promotes the layering of In islands [**32**]. On further annealing the single monolayer covered Si (113) surface at 600^{o}C, it was observed that most of the indium atoms desorbed from the surface while 2D-islands having an average size of 4±0.3 nm and density of 4 E12 cm^{-2} remains on the surface (**Fig. 4(f)**). The complete desorption of In atoms from Si (113) surface took place at 620 °C and a clean reconstructed Si (113) 3x2 surface was obtained [exactly similar to **Fig. 2(a)**]. The complete desorption temperature of In atoms on Si (113) surface is found to be in between the reported desorption temperature on planar Si (111) (570 ^{o}C) and high-index trenched Si (5512) (820^{o}C) [**16**] surfaces. Higher desorption temperature than planar (111) surface clearly indicates a stronger bonding between adsorbate and substrate atoms in a high-index surface owing to better coordination. This may be ascribed to the terrace and stepped-type morphology of the Si (113) surface, furnished with intermediate dangling bond density and hence providing stability to In atoms. On annealing the Si (113) surface beyond 620 °C, 3x2 reconstruction reappeared on the surface.

A consolidate size and density of the In NCs developed at different annealing temperatures has been tabulated in **Table 1**. RT deposited Si (113) surface covered In-NCs are completely converted to comparatively flat surface by annealing up to 200^{o}C. The average size of the NCs has been reduced from 6 ±0.3 to 2±0.3 nm. On further annealing metastable state of SNCs was observed with average size and density of 10±0.3 nm and 2x10^{12} cm^{-2} respectively. Annealing at 500^{o}C, NCs of average size 2±0.3 nm was observed which is similar to the size obtained at 200^{o}C annealing temperature. Beyond this temperature at 600^{o}C, 1 ML covered In flat layer nuclide into tiny nano-islands with average size of 4±0.3 nm. Interestingly, in the present study of In/Si (113) system, a competition between layer and nano-cluster rearrangement has been observed twice during the entire thermal desorption process (both before bilayer & monolayer desorption) which suggests that the surface morphology play significant role in defining the stability of the layers and desorption pathways of adsorbed In atoms from the surface.

Conclusion

In this work, the phenomena of layering to nano-clustering and vice versa of In atoms on reconstructed Si (113) 3x2 surface has been studied by means of STM while XPS study is utilized for the elemental analysis of Si (113) surface. The atomically resolved thermally stable Si (113) surface (inset of **Fig. 2a**) was observed after the in-situ cleaning procedure with stable 3x2 reconstructions. Initial In deposition on Si (113) surface forms small size In NCs with average size of 6±0.3 nm. Controlled thermal desorption analysis divulged the formation of In 3D-SNCs with a maximum size of 10±0.3 nm. A competition between layer to cluster rearrangement has been observed twice during the entire thermal desorption process and the complete desorption of In atoms from Si (113) was observed at 620°C. The outcomes of the current study contribute to the fundamental understanding of growth kinetics, phenomenon of nucleation and segregation of Indium nano-islands on reconstructed Si (113) surface. Further, the size tunability of metallic (In) NCs can be utilized for controlled epitaxy as well as fabrication of next generation nanoscale devices.

Acknowledgements

The authors gratefully acknowledge Professor R. C Budhani, Director, CSIR-NPL, New Delhi for his constant encouragement and support. The work is supported by CSIR-TAPSUN Network Project (NWP-55); Inorganic Light Emitting Diode. One of the Author (SKTC) is grateful to the Department of Science and Technology (DST) and SIMCO Global Technology & System Ltd. for providing Prime Minister Doctoral Fellowship.

Reference

1. Schmid, G.; Bäumle, M.; Geerkens, M.; Heim, I.; Osemann, C.; Sawitowski, T.; *Chem Soc Rev.* **1999**, *28*, 179. **DOI:** 10.1039/A801153B
2. Koplin, E.; Simon, U.; *Met. Nanoclusters Catal. Mater. Sci.: Issue Size Control* **2008**, 107.

3. Ueno, K.; Takabatake, S.; Onishi, K.; Itoh, H.; Nishijima, Y.; Misawa, H.; *Appl. Phy. Lett.* **2011**, *99*, 011107. **DOI:** 10.1063/1.3606505
4. Cuenat, A.; George, H.B.; Chang, K.C.; Blakely, J.M.; Aziz, M.J.; *Adv. Mater.* **2005**, *17*, 2845. **DOI:** 10.1002/adma.200500717
5. Chimmalgi, A.; Grigoropoulos, C.P.; Komvopoulos, K. J.; *Appl. Phys. Lett.* **2005**, *97*, 104319. **DOI:** 10.1063/1.1899245
6. Facsko, S.; Dekorsy, T.; Koerdt, C.; Trappe, C.; Kurz, H.; Vogt, A.; Hartnagel, H.L.; *Science* **1999**, *285*, 1551. **DOI:** 10.1126/science.285.5433.1551
7. Nogami, J.; Park, S.; Quate, C.F.; *Phys. Rev. B* **1987**, 36, 6221. **DOI:** 10.1103/PhysRevB.36.6221
8. Chen, Y.; Ohlberg, D.A.A.; Medeiros-Ribeiro, G.; Chang, Y.A.; Williams, R.S.; *Appl. Phys. Lett*. **2000**, *76*, 4004. **DOI:** 10.1063/1.126848
9. Shang, L.; Shaojun, D.; Ulrich Nienhaus, G.; *Nanotoday* **2011**, *6*, 401. **DOI:** 10.1016/j.nantod.2011.06.004
10. Tsai, T.C.; Lou, L.R.; Lee, C.T.; J. *Nanosci. Nanotechnol.* **2011**, *11*, 6837.
11. Santhana, R.P.; Nair, K.G.M.; Kesavamoorthy, R.; Panigrahi, B.K.; Dhara, S.; Ravichandran, V.; *Appl. Phys. A* **2007**, *87*, 709. **DOI:** 10.1007/s00339-007-3867-2
12. Shibin Krishna, T.C.; Deshmukh, R.; Chauhan, A.K.S.; Goswami, L.; Govind. *Mater. Res. Express*. **2014**, *1*, 015909. **DOI:** 10.1088/2053-1591/1/1/015909
13. Kumar, M.; Govind. *J. Nanopart. Res*. **2012**, *14*, 963. **DOI:** 10.1007/s11051-012-0963-9
14. Waser, R. Nanoelectronics and Information Technology, *Advanced Electronic Materials and Novel Devices* **2003** (Weinheim: Wiley-VCH)
15. Chauhan, A. K. S.; Eldosea, N. M.; Mishra, M.; Niazib, A.; Nair, L.; Gupta, G.; *Appl. Surf. Sci*. **2014**, 314. **DOI:** 10.1016/j.apsusc.2014.06.163
16. Kuyyalil, J.; Govind; Kumar, M.; Shivaprasad, S.M.; *Surf. Sci.* **2010**, *604*, 1972. **DOI:** 10.1016/j.susc.2010.08.006
17. Knall, J.; Pethica, J. B.; *Surf. Sci.* **1992**, *265*, 156. **DOI:** 10.1016/0039-6028(92)90496-S
18. Keller, S.; Heikman, S.; Ben-Yaacov, I.; Shen, L.; DenBaars, S. P.; Mishra, U. K.; *Appl. Phys. Lett.* **2001**, *79*, 3449. **DOI:** 10.1063/1.1420573
19. Gogneau, N.; Sarigiannidou, E.; Monroy, E.; Monnoye, S.; Mank, H.; Daudin, B.; *Appl. Phys. Lett.* **2004**, *85*, 1421. **DOI:** 10.1063/1.1782264
20. Mino, M.; Nakahara, H.; Saito, Y.; Suzuki, H.; *e-J. Surf. Sci. Nanotech.* **2008**, *6*, 45. **DOI:** 10.1380/ejssnt.2008.45
21. Irokawa, K.; Nagura, Y.; Kobayashi, H.; Hara, S.; Fujishiro, H.I.; Miki, H.; Kawazu, A.; Watanabe, K.; *Surface Science* **2009**, *603*, 1197. **DOI:** 10.1016/j.susc.2009.02.036
22. Enta, Y.; Suzuki, S.; Kono, S.; Sakamoto, T.; *Phys. Rev. B.* **1989**, *39*, 5524. **DOI:** 10.1103/PhysRevB.39.5524
23. Dijken, S.van; Zandvliet, H.J.W.; Poelsema, B.; *Phys. Rev. B.* **1997**, *55*, 7864. **DOI:** 10.1103/PhysRevB.55.7864
24. Lee, G.D.; Yoon, E.; *Phys. Rev. B*. **2003**, *68*, 113304. **DOI:** 10.1103/PhysRevB.68.113304
25. Knall, J.; Pethica, J.B.; Todd, J.B.; Wilson, J.H.; *Phys. Rev. Lett.* **1991**, *66*, 1733. **DOI:** 10.1103/PhysRevLett.66.1733
26. Sakama, H.; Kunimatsu, D.; Kageshima, M.; Kawazu, A.; *Phys. Rev. B.* **1996**, *53*, 6927. **DOI:** 10.1103/PhysRevB.53.6927
27. Irokawa, K.; Nagura, Y.; Kobayashi, H.; Hara, S.; Fujishiro, H.I.; Miki, H.; Kawazu, A.; Watanabe, K.; *Surf. Sci.* **2009**, *603*, 1197. **DOI:** 10.1016/j.susc.2009.02.036
28. Lee, G.D.; Yoon, E.; *Surf. Sci.* **2004**, *559*, 63. **DOI:** 10.1016/j.susc.2009.02.036
29. Schreiner, J.; Jacobi, K.; Selke, W.; *Phys. Rev. B.* **1994**, *49*, 2706. **DOI:** 10.1103/PhysRevB.49.2706
30. Siebert, M.; Schmidt, T.; Flege, J.I.; Falta, *J.*; *Phys. Rev. B.* **2005**, *72*, 045323. **DOI:** 10.1103/PhysRevB.72.045323
31. Tangi, M.; Kuyyalil, J.; Shivaprasad, S.M.; *J. Appl. Phys*. **2013**, *114*, 153501. **DOI:** 10.1063/1.4824823
32. Jithesh, K.; Govind; Kumar, M.; Shivaprasad, S.M.; *J. Nanosci. Nanotech.* **2009**, *9*, 5417.
33. Goswami, D.K.; Battacharjee, K.; Satpati, B.; Roy, S.; Satyam, P.V.; Dev, B.N.; *Surf. Sci*. **2007**, 601. **DOI:** 10.1016/j.susc.2006.10.026